

Quantum state truncation using an optical parametric amplifier and a beamsplitter

E.P. Mattos and A. Vidiella-Barranco ¹

Gleb Wataghin Institute of Physics - University of Campinas
13083-859 Campinas, SP, Brazil

Abstract

We present a scheme of quantum state truncation in the Fock basis (quantum scissors), based on the combined action of a nondegenerate optical parametric amplifier and a beamsplitter. Differently from previously proposed linear-optics-based quantum scissors devices, which depend on reliable Fock states sources, our scheme requires only readily available Gaussian states, such as coherent states inputs (vacuum state included). A truncated state is generated after performing photodetections in the global state. We find that, depending on which output ports each of the two photodetectors is positioned, different types of truncated states may be produced: i) states having a maximum Fock number of N , or ii) states having a minimum Fock number N . In order to illustrate our method, we discuss an example having as input states a coherent state in the beamsplitter and vacuum states in the amplifier, and show that the resulting truncated states display nonclassical properties, such as sub-Poissonian statistics and squeezing. We quantify the nonclassicality degree of the generated states using the Wigner-Yanase skew information measure. For complementarity, we discuss the efficiency of the protocol, e.g., generation probability as well as the effects of imperfections such as the detector's quantum efficiency and dark counts rate.

1 Introduction

The engineering of quantum states of light has experienced extraordinary progress in recent years [1]. Despite the fact that the photon concept emerged in the early days of quantum theory, the generation of pure photon number states, or Fock states $|n\rangle$, has been particularly challenging. Early attempts to generate, for instance, single photon states to some degree of control occurred only in the 1970s, using nonlinear media, [2] or in atomic systems [3]. This was well after the generation of coherent states (laser light) in the 1960s [4], and before the successful production of squeezed states of light [5]. Since those pioneering experiments, there have been considerable efforts to generate states of light having diverse nonclassical properties [1, 6], also because they are essential resources for the development of quantum technologies [6–8]. Amongst the proposed methods, we may cite quantum state engineering schemes using arrays of beamsplitters with injection of suitable states (usually Fock states) followed by photodetections [9]. There are also proposals based on the use of specifically engineered nonlinear media [10, 11], as well as in cavity QED systems [12–14]. Needless to say it is worth looking for alternative generation schemes, since quantum states engineering protocols are in general not easy to implement.

An appealing approach is to try to modify an already existing state of light by applying some kind of operation on it. As examples of such operations we could cite: photon addition [15], photon subtraction [16], and the removal of specific components in the Fock basis (“hole burning”) [17]. We remark that the removal of

¹vidiella@ifp.unicamp.br

the vacuum state is enough to transform an arbitrary state into a nonclassical one, as discussed in [18]. Another interesting procedure is the so-called quantum state truncation, also known as “quantum scissors” after reference [19]. A quantum scissors device transforms a quantum state of light, say $|\varphi\rangle$, into a state having a finite number of Fock components, that can be a superposition of the vacuum state $|0\rangle$ and the one photon state $|1\rangle$: $\hat{T}|\varphi\rangle = c_0|0\rangle + c_1|1\rangle$. We note that the truncation of quantum states in the Fock basis can also be performed in vibrational states of a trapped ion system [20]. A typical quantum scissors device for light [19] consists of two beamsplitters placed side by side, having the vacuum state $|0\rangle$ and a single photon Fock state $|1\rangle$ as input states of the first beamsplitter, and an arbitrary state $|\varphi\rangle$ as input state of the second beamsplitter. The other input of the second beamsplitter is precisely the transmitted output of the first beamsplitter. Two photodetectors are placed in the output ports of the second beamsplitter, and the detection of one photon in one and no photons in the other projects the reflected output of the first beamsplitter into a truncated state [19]. Such a process is allowed because the quantum state $|\varphi\rangle$ is mixed with an entangled state (involving the vacuum state $|0\rangle$ and a single photon state $|1\rangle$) in the second beamsplitter. We stress that in general, quantum scissors schemes require the injection of Fock states [19, 21, 22], i.e., the prior generation of a highly nonclassical state. In recent years, there has been renewed interest in the study of quantum state truncation. In particular, one can find in the literature a number of works about possible applications, such as: entanglement improvement [23, 24], continuous variable quantum key distribution [25], quantum repeaters, [26], and noiseless amplification [22, 27].

Here we propose a hybrid quantum scissors scheme employing linear (beamsplitter) and nonlinear (nondegenerate optical parametric amplifier) devices, as displayed in Fig. 1. We show that, in our method, truncated states may be generated in a straightforward way without having to resort to Fock states as inputs. Rather, it is sufficient to have vacuum states entering the amplifier input ports and a coherent state as input to the beamsplitter. We also show that it is possible to generate two distinct classes of truncated states simply by placing the photodetectors in different exit ports. Furthermore, our alternative scheme offers additional possibilities for the output states, depending on the strength and phase of the parametric amplifier.

This paper is organized as follows: In Section 2 we present our nonlinear-linear quantum scissors. In Section 3 we study a specific example of truncated state generation using Gaussian states inputs. We also discuss some nonclassical properties as well as the degree of nonclassicality of the generated states using the Wigner-Yanase skew information [28, 29]. The efficiency of the protocol taking into account imperfections in the photodetections is analysed in Section 4, and in Section 5 we conclude our work.

2 A scheme for generalized quantum state truncation

Our proposal is based in sequential interactions using the setup shown in Fig.1. It employs a nonlinear device, namely a nondegenerate optical parametric amplifier placed besides a linear device, a beamsplitter, in such a way that one of the amplifier’s output ports (along mode \hat{b} , see Fig. 1) becomes one of the beamsplitter’s input modes. The other input port of the beamsplitter (mode \hat{c}) is fed by an arbitrary quantum state of light. Photodetectors may be placed in two output ports, out of the three existing ones. We consider two configurations: i) both photodetectors in the two output ports of the beamsplitter (\hat{b}_{out} and \hat{c}_{out} modes), or ii) one photodetector

in an output port of the beamsplitter (\hat{c}_{out} mode) and the other in the remaining output port of the amplifier (\hat{a}_{out} mode). Naturally, the generated quantum state of light, conditioned to the corresponding photodetections, will come out through the port which has been left open. As we are going to see below, different families of nonclassical states can be generated, depending on the positions in which the detectors are placed.

We consider a simple case, in which the initial state entering the amplifier/beamsplitter device is such that both input modes of the amplifier are in the vacuum state, and the input mode \hat{c} (beamsplitter) is in a generic pure state $|\psi\rangle = \sum \psi_i |i\rangle$, or

$$|\Psi_{in}\rangle = \sum_{i=0}^{\infty} \psi_i |0, 0, i\rangle, \quad (1)$$

where $|0, 0, i\rangle \equiv |0\rangle_a \otimes |0\rangle_b \otimes |i\rangle_c$. The combined action of the amplifier and beamsplitter on the initial state $|\Psi_{in}\rangle$ may be represented as

$$|\Phi_{out}\rangle = \hat{R}(\theta) \hat{S}(\xi) |\Psi_{in}\rangle, \quad (2)$$

being $\hat{S} = \exp[\xi^* \hat{a} \hat{b} - \xi \hat{a}^\dagger \hat{b}^\dagger]$ the two-mode squeezing operator and $\hat{R} = \exp[i\theta(\hat{a}^\dagger \hat{b} + \hat{a} \hat{b}^\dagger)]$ the operator associated to the beamsplitter action. The relevant parameters here are $\xi = s e^{i\phi}$, where s is basically the strength of the amplifier ($s \geq 0$), and ϕ is the phase of the pump field (treated as classical here). The parameter θ is related to the (complex) transmittance T and reflectance R of the beamsplitter ($|T|^2 + |R|^2 = 1$). After some algebra (see details in the Appendix), the output state prior to the photodetections will read

$$\begin{aligned} |\Phi_{out}\rangle &= \sum_{i=0}^{\infty} \sum_{n=0}^{\infty} \sum_{j=0}^i \sum_{m=0}^n \frac{\sqrt{i!}}{j!(i-j)!} \frac{\sqrt{n!}}{m!(n-m)!} \sqrt{(i-j+n-m)!} \sqrt{(j+m)!} \psi_i A_n(s, \phi) \\ &\times T^j T^{*n-m} R^m (-R^*)^{i-j} |n, i-j+n-m, j+m\rangle, \end{aligned} \quad (3)$$

with $A_n(s, \phi) = \text{sech } s (-e^{i\phi} \tanh s)^n$.

2.1 Photon detectors placed in both the beamsplitter's output ports

If the photodetectors are placed in such a way that one is at \hat{b}_{out} and the other at \hat{c}_{out} , having one photon detected in \hat{b}_{out} and no photons detected in \hat{c}_{out} , the following conditional truncated state will be generated in mode \hat{a}_{out}

$$|\Phi_a^{(1,0)}\rangle = -\frac{1}{\sqrt{p_a^{(1,0)}}} \text{sech } s (\psi_1 R^* |0\rangle + \psi_0 e^{i\phi} \tanh s T^* |1\rangle), \quad (4)$$

with

$$p_a^{(1,0)} = \text{sech}^2 s (|R|^2 |\psi_1|^2 + |T|^2 |\psi_0|^2 \tanh^2 s). \quad (5)$$

The state in Eq. (4), a quantum superposition of the vacuum state and the one-photon state, has the form of a typical truncated state obtained via a conventional quantum scissors device [19]. We remind the reader that in the quantum scissors schemes previously discussed in the literature, states which are difficult to generate in a controlled way (Fock states) are required as input states. In our method there is no need of previous generation of Fock states; the input states in the amplifier are simply vacuum states (apart from the classical pump), with an arbitrary state $|\psi\rangle$ entering the beamsplitter's port \hat{c} .

It is possible to generalize the result above for N photons being detected in \hat{b}_{out} and no photons in \hat{c}_{out} . In this case the generated state will be

$$|\Phi_a^{(N,0)}\rangle = \frac{1}{\sqrt{p_a^{(N,0)}}} \text{sech } s \sum_{n=0}^N \sqrt{\frac{N!}{n!(N-n)!}} \psi_{N-n} (-e^{i\phi} \tanh s)^n \mathbf{T}^{*n} (-\mathbf{R}^*)^{N-n} |n\rangle, \quad (6)$$

with

$$p_a^{(N,0)} = \text{sech}^2 s \sum_{n=0}^N \frac{N!}{n!(N-n)!} |\psi_{N-n}|^2 |\mathbf{T}|^{2n} |\mathbf{R}|^{2(N-n)} \tanh^{2n} s. \quad (7)$$

In other words, our scheme allows, in principle, the generation of a truncated state up to Fock number N .

We note that Fock states as well as the vacuum state can also be output states of the quantum scissors device for particular values of the transmittance. From Eq. (4) it follows that if $|\mathbf{T}| = 1$ a one photon state $|1\rangle$ is generated, while if $|\mathbf{T}| = 0$, the resulting state in \hat{a}_{out} will be simply the vacuum state.

2.2 Photon detectors placed in the beamsplitter's and amplifier's output ports

In this case the photodetectors will be placed in the ports corresponding to the \hat{a}_{out} (amplifier) and \hat{c}_{out} (beamsplitter) modes. For instance, if one photon is recorded at the amplifier output and no photon is detected at the beamsplitter output, the generated state at port \hat{b}_{out} will be

$$|\Phi_b^{(1,0)}\rangle = \frac{1}{\sqrt{p_b^{(1,0)}}} \text{sech } s (-e^{i\phi} \tanh s) \mathbf{T}^* \sum_{i=0}^{\infty} \sqrt{i+1} \psi_i (-\mathbf{R}^*)^i |i+1\rangle, \quad (8)$$

with

$$p_b^{(1,0)} = \text{sech}^2 s \tanh^2 s |\mathbf{T}|^2 \sum_{i=0}^{\infty} (i+1) |\psi_i|^2 |\mathbf{R}|^{2i}. \quad (9)$$

Note that the vacuum component $|0\rangle$ has been removed from the state in Eq. (8), i.e., the states of the type $|\Phi_b^{(1,0)}\rangle$ are nonclassical [18].

Again, we may generalize the above result if N photons are recorded at the amplifier's output port (mode \hat{a}_{out}) and no photon is recorded at the beamsplitter port. In this case, the generated state will read

$$|\Phi_b^{(N,0)}\rangle = \frac{1}{\sqrt{p_b^{(N,0)}}} \text{sech } s (-e^{i\phi} \tanh s)^N \mathbf{T}^{*N} \sum_{i=0}^{\infty} \sqrt{\frac{(i+N)!}{i!N!}} \psi_i (-\mathbf{R}^*)^i |i+N\rangle \quad (10)$$

with

$$p_b^{(N,0)} = \text{sech}^2 s \tanh^{2N} s |\mathbf{T}|^{2N} \sum_{i=0}^{\infty} \frac{(i+N)!}{i!N!} |\psi_i|^2 |\mathbf{R}|^{2i}. \quad (11)$$

Thus, such scheme makes possible to generate states truncated from Fock number N , i.e., all components having $n < N$ being null.

Interestingly, the two different photodetectors placements discussed lead to the generation of states that are somehow ‘‘complementary’’: in Section 2.1 we showed how states with a maximum Fock number N can be generated, and here in Section 2.2, we saw that it is also possible to generate states having a minimum Fock number N .

3 State generation from coherent states: nonclassical properties

We may use the parametrization $T = \cos \theta$ and $R = i \sin \theta$, so that we are left with three parameters: (s, ϕ) , which are related to the amplifier/pump, and θ , related to the beamsplitter's transmittance. This gives a great flexibility to our generation scheme, since we can tune the properties of the generated states by changing experimentally controlled parameters. Now we would like to illustrate our method by choosing specific input states (mode \hat{c}), namely, the "quasi-classical" coherent states $|\psi\rangle = |\alpha\rangle$, with $\alpha = |\alpha|e^{i\beta}$. In this case the truncated states $|\Phi_a^{(N,0)}\rangle$ (and their properties), will depend on the phase difference $\phi - \beta$, as one can see in Eq. (6).

3.1 Sub-Poissonian statistics

A well-known measure of photon number fluctuations is the Mandel Q parameter, defined as $Q = \langle (\Delta \hat{n})^2 \rangle / \langle \hat{n} \rangle - 1$. It has a minimum value of $Q = -1$ for Fock states, and is null for coherent states, i.e., it indicates deviations from the characteristic Poissonian photon statistics of a coherent state. We firstly analyze the occurrence of sub-Poissonian statistics of the generated truncated state $|\Phi_a\rangle$ discussed in Section 2.1. To begin with, we may set $|\alpha| = 1$, $\phi - \beta = \pi/2$ rad, $\theta = \pi/4$ rad (a 50 : 50 beamsplitter) and vary the strength s . The result, in Fig. 2 (for different values of N), shows that the generated states exhibit sub-Poissonian statistics. If we now set the parameters $s = 0.5$, $\phi - \beta = \pi/2$ rad and vary θ , we obtain the results shown in Fig. 3, i.e., the generated states are also mostly sub-Poissonian. The states discussed in Section 2.2, $|\Phi_b\rangle$, may also exhibit sub-Poissonian statistics, although in a lesser degree than the states $|\Phi_a\rangle$.

In our scheme, energy is injected into the system via both the classical pump and the input field (mode \hat{c}). We therefore expect that the nonclassical properties of the output field will depend on s , as well as on α (in case of a coherent state input). In Fig. 4 we have a plot of Mandel's Q parameter as a function of s and $|\alpha|$, for the state $|\Phi_a\rangle$ with $N = 1$. We note that for larger values of $|\alpha|$ the output state is driven onto a Poissonian state. Yet, small values of $|\alpha|$ combined with a not too weak pumping favors the generation of sub-Poissonian states.

3.2 Quadrature squeezing

Another important nonclassical feature to be discussed is the so-called squeezing; the reduction of fluctuations in the quadrature variables below the characteristic value of a coherent state. For instance, if $\langle (\Delta \hat{X})^2 \rangle < 1/4$ the quadrature \hat{X} , defined as $\hat{X} = (\hat{a} + \hat{a}^\dagger)/2$, is said to be squeezed. The truncated states $|\Phi_a\rangle$ may exhibit squeezing in the \hat{X} quadrature for $\phi - \beta = \pi/2$ rad and $\theta = \pi/4$ rad, as shown in Fig. 5, where the variance of \hat{X} is plotted as a function of s . Squeezing may also be present for different combinations of the involved parameters, as it is evident from the plots of $\langle (\Delta \hat{X})^2 \rangle$ as a function of $\phi - \beta$ (Fig. 6), with $\theta = \pi/4$ rad, as well as a function of θ (Fig. 7), with $\phi - \beta = \pi/2$ rad. In both cases $s = 0.5$, and squeezing occurs for ranges of values of $\phi - \beta$ (or θ). The states $|\Phi_b\rangle$ may also exhibit squeezing.

Squeezing in the truncated state $|\Phi_a\rangle$ depends not only on the pump strength s but also on the input state amplitude, α . As clearly shown in Fig. 8, combinations of values of s and $|\alpha|$, may yield significant amounts of squeezing to the generated states.

3.3 Nonclassicality

Properties such as sub-Poissonian statistics and squeezing capture different nonclassical aspects of quantum states of light. Nonetheless, due to the multi-sided nature of quantumness (nonclassicality), it is not an easy task to find a quantity that would contain as much information as possible about the nonclassical character of a quantum state. So far, we have witnessed efforts to quantify nonclassicality from different perspectives and, as a consequence, several figures of merit have been introduced for this purpose. We may find in the literature works discussing various nonclassicality criteria, e.g., distance-based measures [30], nonclassical depth [31], quadrature-based measures [32, 33], negativity of phase space distributions [34] and operator ordering sensitivity [35]. A recently introduced and interesting information-theoretic nonclassicality quantifier is the Wigner-Yanase skew information [28, 29]. For a pure, single mode state of the electromagnetic field $|\Psi\rangle$, the skew information is given by [28]

$$W(|\Psi\rangle) = \frac{1}{2} + \langle \Psi | \hat{a}^\dagger \hat{a} | \Psi \rangle - \langle \Psi | \hat{a}^\dagger | \Psi \rangle \langle \Psi | \hat{a} | \Psi \rangle. \quad (12)$$

Among other interesting properties, the skew information is non-negative and for pure states has a minimum value of $W_{min} = 1/2$ (coherent states). Also, larger values of W indicate a larger nonclassical character of a given state [28]. We evaluated the skew information W for the states generated in our scissors device. For instance, in Fig. 9 we have plotted W as a function of s for the states $|\Phi_a\rangle$ setting $\phi - \beta = \pi/2$ rad and $\theta = \pi/4$ rad. We note that the skew information is an increasing function of s , which can be associated to an increasing sub-Poissonian character (see Fig. 2). Also in this case there are variable levels of squeezing, as seen in Fig. 5, i.e., W captures an overall nonclassical behavior of those states. We could also set $s = 0.5$, $\phi - \beta = \pi/2$ rad and vary θ . The resulting plots are shown in Fig. 10. Thus, the Wigner-Yanase skew information captures the nonclassical character of the generated states, and it can be associated to sub-Poissonian statistics and/or squeezing. Besides, as it is clearly seen in the graphs, the nonclassical character is more pronounced for states having a higher maximum Fock number N .

4 Efficiency of the protocol

Quantum scissors rely on photodetections, and hence perform quantum state truncation non-deterministically. Therefore, even under ideal conditions, success probabilities may be associated to its realization. Besides, photodetectors are imperfect, which certainly has a negative impact on the quality of the generated states. In what follows we are going to discuss some aspects of the efficiency of our scheme.

4.1 Generation probabilities

The probability of generation of state $|\Phi_a^{(N,0)}\rangle$, that is, $p_a^{(N,0)}$, is given by Eq.(7) in Section 2.1. It basically depends on θ , s and the coefficients ψ_i (actually $|\psi_i|^2$). Again, we consider for simplicity a coherent state input $|\alpha\rangle$ and a 50 : 50 beamsplitter ($\theta = \pi/4$ rad). We may gauge the dependence of the probability of generation on the modulus of the coherent amplitude, $|\alpha|$, as well as the amplifier strength s by plotting $p_a^{(N,0)}$ as a function of these quantities. This is shown in Fig. 11 for $N = 1$ and in Fig. 12 for $N = 3$. Clearly there are

optimum values of $|\alpha|$ and s that maximize $p_a^{(N,0)}$ for a given N . Naturally, for $N = 3$ there is a substantial drop in the probability of generation, compared to $N = 1$, while the maximum value of $p_a^{(3,0)}$ occurs for slightly larger values of both $|\alpha|$ and s , as we see in the figures.

4.2 Nonideal photodetection

Despite the advances regarding the quality of photodetectors, those devices are still not perfect. Some incoming photons may not be recorded (quantum efficiency is not 100%), and sometimes detectors are spuriously activated (dark counts). We assume that photon-number-resolving detectors (PNRD) are employed, and counts up to N photons are feasible [36]. The imperfections of a single detector can be suitably modeled via the following POVM, [21, 37]

$$\hat{\Pi}_N = \sum_{n=0}^N \sum_{m=n}^{\infty} \frac{e^{-\nu} \nu^{N-n}}{(N-n)!} \eta^n (1-\eta)^{m-n} C_n^m |m\rangle\langle m|, \quad (13)$$

where η is the detector's quantum efficiency, ν the dark count probability, and C_n^m are binomial coefficients. In the setup we are considering here, the action of each one of the detectors will be modeled by $\hat{\Pi}_0$ and $\hat{\Pi}_N$ for zero and for N photon counts, respectively. We assume the same efficiency η and dark count rate ν for both detectors. Due to these imperfections, the generated field should be represented by a density operator, calculated by tracing over the detected modes. If the detectors are placed in output ports \hat{b}_{out} and \hat{c}_{out} , the resulting state will be,

$$\hat{\rho}_a^{(\eta,\nu)} = \mathcal{A} \text{Tr}_{b,c} \left[\hat{\Pi}_0 \hat{\Pi}_N |\Phi_{out}\rangle\langle\Phi_{out}| \right], \quad (14)$$

where $|\Phi_{out}\rangle$ is the state in Eq. (3) and \mathcal{A} is a normalizing constant.

The performance of the protocol may be assessed by calculating the fidelity F of the output state in relation to state $|\Phi_a^{(N,0)}\rangle$ (ideal output state), or

$$F = \langle\Phi_a^{(N,0)}|\hat{\rho}_a^{(\eta,\nu)}|\Phi_a^{(N,0)}\rangle. \quad (15)$$

We proceed by numerically computing the fidelity as a function of $|\alpha|$ and s , for different values of N , which is shown in Figs. 13 and 14, respectively. Firstly, we note that although the fidelity is clearly affected by the detection imperfections, it is possible to generate truncated states with $F \gtrsim 0.9$. Thus, our modified scissors can, in principle, have a robustness against imperfections comparable to that of conventional scissors. Nevertheless, we observe that while in the conventional scissors (with coherent state input) the fidelity F decreases with increasing $|\alpha|$ [21], in our modified scissors F increases with $|\alpha|$ instead, as seen in Fig. 13. On the other hand, the fidelity decreases with increasing pump strength s , as shown in Fig. 14. This behavior can be understood if we take a closer look at the structure of the states generated by each type of scissors. Consider for simplicity the particular case of having 50 : 50 beamsplitters and $N = 1$. In a conventional scissors, the truncated state generated from a coherent state $|\alpha\rangle$ (α real) is of the form $|\varphi\rangle = \mathcal{N}(|0\rangle + \alpha|1\rangle)$, i.e., the coefficient of the one-photon state is simply α . In our modified scissors though, the resulting state is given by $|\varphi'\rangle = \mathcal{N}'(\alpha|0\rangle + \tanh s|1\rangle)$, and the coefficient of the one-photon state is $\tanh s$. Therefore, increasing the value of α (s) in conventional (modified) scissors has the effect of decreasing the fidelity. Conversely, α is the coefficient of the vacuum state in the modified scissors output state and thus, increasing α should have the opposite effect in this case, that is, an increase of the fidelity.

5 Conclusion

We proposed a scheme which allows quantum state truncation via the combined action of a nondegenerate optical parametric amplifier and a beamsplitter. This makes possible to perform the state truncation without the previous generation of Fock states. In fact, there is no need of nonclassical input states whatsoever, and Gaussian states such as vacuum states + coherent states are sufficient resources to generate truncated output states which are nonclassical. This is clearly advantageous, given that the experimental setup can be substantially simplified. We should point out that a single pumped nondegenerate parametric amplifier having vacuum states as inputs, generates a two-mode squeezed vacuum state as an output field. In our scheme, one of the modes of such an entangled state is mixed with an arbitrary field in a beamsplitter, and after the photodetections, the remaining field mode is collapsed onto a truncated state. Accordingly, a nonclassical resource appropriate for state truncation is provided by the operation of the parametric amplifier itself, a device already integrating the proposed arrangement.

Differently from the conventional scissors [19], in our modified quantum scissors the nonclassical properties of the generated states can be selected by changing not only the transmittance of the beamsplitter, but also by adjusting the quantities associated to the classical pump in the amplifier, the strength s and phase ϕ . We should also point out that depending on the position of the photodetectors, different classes of states can be produced. If the photodetectors are placed in both output ports of the beamsplitter, a state having a maximum Fock number, say N , is generated. However, if one photodetector is placed in one of the beamsplitter's port and the other in the amplifier's output port, the generated state will have the Fock components $n < N$ removed. In other words, the scheme presented here allows the generation of states truncated in complementary sections of the Fock basis. Our results are expected to be relevant for exploring novel possibilities involving the combination of linear and nonlinear devices, aiming the manipulation of quantum states of light.

Acknowledgments

E.P.M. would like to acknowledge financial support from CAPES (Coordenadoria de Aperfeiçoamento de Pessoal de Nível Superior), Brazil, grant N^o 88887.514500/2020-00. This work was also supported by CNPq (Conselho Nacional para o Desenvolvimento Científico e Tecnológico, Brazil), via the INCT-IQ (National Institute for Science and Technology of Quantum Information), grant N^o 465469/2014-0.

Appendix A: The derivation for Eq. (3)

We assume for the device in Fig. 1 a joint input state having vacuum states in the amplifier's input ports and an arbitrary pure state $|\psi\rangle = \sum \psi_i |i\rangle$ in the beamsplitter's input port. Thus, the combined action of the amplifier/beamsplitter $\hat{R}(\theta)\hat{S}(\xi)|\Psi_{in}\rangle$, will be

$$|\Phi_{out}\rangle = \hat{R}(\theta)\hat{S}(\xi)|\Psi_{in}\rangle = \sum_{i=0}^{\infty} \frac{1}{\sqrt{i!}} \psi_i \hat{R}(\theta)\hat{S}(\xi)\hat{c}^{\dagger i}|0, 0, 0\rangle. \quad (16)$$

Using now the following relations,

$$\begin{aligned}
\hat{S}\hat{a}^\dagger\hat{S}^\dagger &= \hat{a}^\dagger \cosh s + \hat{b}e^{-i\phi} \sinh s, \\
\hat{S}\hat{b}^\dagger\hat{S}^\dagger &= \hat{b}^\dagger \cosh s + \hat{a}e^{-i\phi} \sinh s, \\
\hat{S}\hat{c}^\dagger\hat{S}^\dagger &= \hat{c}^\dagger, \\
\hat{S}|0,0,0\rangle &= \sum_{n=0}^{\infty} \operatorname{sech} s (-e^{i\phi} \tanh s)^n |n, n, 0\rangle,
\end{aligned} \tag{17}$$

for the squeezing operator, and

$$\begin{aligned}
\hat{R}\hat{a}^\dagger\hat{R}^\dagger &= \hat{a}^\dagger, \\
\hat{R}\hat{b}^\dagger\hat{R}^\dagger &= \mathbf{T}^*\hat{b}^\dagger + \mathbf{R}\hat{c}^\dagger, \\
\hat{R}\hat{c}^\dagger\hat{R}^\dagger &= -\mathbf{R}^*\hat{b}^\dagger + \mathbf{T}\hat{c}^\dagger, \\
\hat{R}|0,0,0\rangle &= |0,0,0\rangle
\end{aligned} \tag{18}$$

for the beamsplitter operator.

Applying the relations above to Eq. (16), we obtain

$$\begin{aligned}
|\Phi_{out}\rangle &= \hat{R}(\theta)\hat{S}(\xi)|\Psi_{in}\rangle = \sum_{i=0}^{\infty} \sum_{n=0}^{\infty} \frac{1}{\sqrt{i!}} \psi_i A_n(\xi) \hat{R}\hat{c}^{\dagger i} |n, n, 0\rangle \\
&= \sum_{i=0}^{\infty} \sum_{n=0}^{\infty} \frac{1}{\sqrt{i!}} \frac{1}{\sqrt{n!}} \psi_i A_n(\xi) \hat{R}\hat{b}^{\dagger n} \hat{c}^{\dagger i} |n, 0, 0\rangle \\
&= \sum_{i=0}^{\infty} \sum_{n=0}^{\infty} \frac{1}{\sqrt{i!}} \frac{1}{\sqrt{n!}} \psi_i A_n(s, \phi) (\mathbf{T}^*\hat{b}^\dagger + \mathbf{R}\hat{c}^\dagger)^n (-\mathbf{R}^*\hat{b}^\dagger + \mathbf{T}\hat{c}^\dagger)^i |n, 0, 0\rangle,
\end{aligned} \tag{19}$$

which results in

$$|\Phi_{out}\rangle = \sum_{i=0}^{\infty} \sum_{n=0}^{\infty} \sum_{j=0}^i \sum_{m=0}^n \frac{1}{\sqrt{i!}} \frac{1}{\sqrt{n!}} \frac{i!}{j!(i-j)!} \frac{n!}{m!(n-m)!} \psi_i A_n(s, \phi) (\mathbf{T}^*\hat{b}^\dagger)^{n-m} (\mathbf{R}\hat{c}^\dagger)^m (-\mathbf{R}^*\hat{b}^\dagger)^{i-j} (\mathbf{T}\hat{c}^\dagger)^j |n, 0, 0\rangle. \tag{20}$$

Finally,

$$\begin{aligned}
|\Phi_{out}\rangle &= \sum_{i=0}^{\infty} \sum_{n=0}^{\infty} \sum_{j=0}^i \sum_{m=0}^n \frac{\sqrt{i!}}{j!(i-j)!} \frac{\sqrt{n!}}{m!(n-m)!} \sqrt{(i-j+n-m)!} \sqrt{(j+m)!} \psi_i A_n(s, \phi) \\
&\times \mathbf{T}^j \mathbf{T}^{*n-m} \mathbf{R}^m (-\mathbf{R}^*)^{i-j} |n, i-j+n-m, j+m\rangle.
\end{aligned} \tag{21}$$

References

- [1] V V Dodonov. Nonclassical states in quantum optics: a squeezed review of the first 75 years. *J. Opt. B*, 4:R1, 2002.
- [2] David C. Burnham and Donald L. Weinberg. Observation of simultaneity in parametric production of optical photon pairs. *Phys. Rev. Lett.*, 25:84, 1970.
- [3] John F. Clauser. Experimental distinction between the quantum and classical field-theoretic predictions for the photoelectric effect. *Phys. Rev. D*, 9:853, 1974.
- [4] T Maiman. Stimulated optical radiation in ruby. *Nature (London)*, 187:493, 1960.
- [5] R. E. Slusher, L. W. Hollberg, B. Yurke, J. C. Mertz, and J. F. Valley. Observation of squeezed states generated by four-wave mixing in an optical cavity. *Phys. Rev. Lett.*, 55:2409–2412, Nov 1985.
- [6] Anirban Pathak and Ajoy Ghatak. Classical light vs. nonclassical light: characterizations and interesting applications. *J. Electromagnet. Waves Appl.*, 32(2):229, 2018.
- [7] Dan Browne, Sougato Bose, Florian Mintert, and M.S. Kim. From quantum optics to quantum technologies. *Prog. Quantum Electron.*, 54:2–18, 2017.
- [8] Stephen M. Barnett, Almut Beige, Artur Ekert, Barry M. Garraway, Christoph H. Keitel, Viv Kendon, Manfred Lein, Gerard J. Milburn, Héctor M. Moya-Cessa, Mio Muraio, Jiannis K. Pachos, G. Massimo Palma, Emmanuel Paspalakis, Simon J.D. Phoenix, Benard Piraux, Martin B. Plenio, Barry C. Sanders, Jason Twamley, A. Vidiella-Barranco, and M.S. Kim. Journeys from quantum optics to quantum technology. *Prog. Quantum Electron.*, 54:19–45, 2017.
- [9] M. Dakna, J. Clausen, L. Knöll, and D.-G. Welsch. Generation of arbitrary quantum states of traveling fields. *Phys. Rev. A*, 59:1658–1661, Feb 1999.
- [10] S. Ya. Kilin and D. B. Horoshko. Fock state generation by the methods of nonlinear optics. *Phys. Rev. Lett.*, 74:5206–5207, Jun 1995.
- [11] A. Vidiella-Barranco and J. A. Roversi. Quantum state engineering via unitary transformations. *Phys. Rev. A*, 58:3349–3352, Oct 1998.
- [12] K. Vogel, V. M. Akulin, and W. P. Schleich. Quantum state engineering of the radiation field. *Phys. Rev. Lett.*, 71:1816–1819, Sep 1993.
- [13] H. Moya-Cessa, P. L. Knight, and A. Rosenhouse-Dantsker. Photon amplification in a two-photon lossless micromaser. *Phys. Rev. A*, 50:1814–1821, Aug 1994.
- [14] C. K. Law and J. H. Eberly. Arbitrary control of a quantum electromagnetic field. *Phys. Rev. Lett.*, 76:1055–1058, Feb 1996.

- [15] G. S. Agarwal and K. Tara. Nonclassical properties of states generated by the excitations on a coherent state. *Phys. Rev. A*, 43:492–497, Jan 1991.
- [16] G. S. Agarwal. Negative binomial states of the field-operator representation and production by state reduction in optical processes. *Phys. Rev. A*, 45:1787–1792, Feb 1992.
- [17] B. M. Escher, A. T. Avelar, T. M. da Rocha Filho, and B. Baseia. Controlled hole burning in the fock space via conditional measurements on beam splitters. *Phys. Rev. A*, 70:025801, Aug 2004.
- [18] Ching Tsung Lee. Theorem on nonclassical states. *Phys. Rev. A*, 52:3374–3376, Oct 1995.
- [19] David T. Pegg, Lee S. Phillips, and Stephen M. Barnett. Optical state truncation by projection synthesis. *Phys. Rev. Lett.*, 81:1604–1606, Aug 1998.
- [20] H. Moya-Cessa and P. Tombesi. Filtering number states of the vibrational motion of an ion. *Phys. Rev. A*, 61:025401, Jan 2000.
- [21] Sahin Kaya Özdemir, Adam Miranowicz, Masato Koashi, and Nobuyuki Imoto. Quantum-scissors device for optical state truncation: A proposal for practical realization. *Phys. Rev. A*, 64:063818, Nov 2001.
- [22] Matthew S. Winnel, Nedasadat Hosseinidehaj, and Timothy C. Ralph. Generalized quantum scissors for noiseless linear amplification. *Phys. Rev. A*, 102:063715, Dec 2020.
- [23] Xuexiang Xu, Liyun Hu, and Zeyang Liao. Improvement of entanglement via quantum scissors. *J. Opt. Soc. Am. B*, 35(1):174–181, Jan 2018.
- [24] Liyun Hu, M. Al-amri, Zeyang Liao, and M. S. Zubairy. Entanglement improvement via a quantum scissor in a realistic environment. *Phys. Rev. A*, 100:052322, Nov 2019.
- [25] M. Ghalaii, C. Ottaviani, R. Kumar, S. Pirandola, and M. Razavi. Discrete-modulation continuous-variable quantum key distribution enhanced by quantum scissors. *IEEE J. Sel. Top. Quantum Electron.*, 26:1, 2020.
- [26] Kaushik P. Seshadreesan, Hari Krovi, and Saikat Guha. Continuous-variable quantum repeater based on quantum scissors and mode multiplexing. *Phys. Rev. Research*, 2:013310, Mar 2020.
- [27] Mingjian He, Robert Malaney, and Benjamin A. Burnett. Noiseless linear amplifiers for multimode states. *Phys. Rev. A*, 103:012414, Jan 2021.
- [28] Shunlong Luo and Yue Zhang. Quantifying nonclassicality via wigner-yanase skew information. *Phys. Rev. A*, 100:032116, Sep 2019.
- [29] E. P. Wigner and Mutsuo M. Yanase. Information contents of distributions. *Proc. Natl. Acad. Sci. USA*, 49(6):910–918, 1963.
- [30] Mark Hillery. Nonclassical distance in quantum optics. *Phys. Rev. A*, 35:725–732, Jan 1987.

- [31] Ching Tsung Lee. Measure of the nonclassicality of nonclassical states. *Phys. Rev. A*, 44:R2775–R2778, Sep 1991.
- [32] Th. Richter and W. Vogel. Nonclassicality of quantum states: A hierarchy of observable conditions. *Phys. Rev. Lett.*, 89:283601, Dec 2002.
- [33] E. Shchukin, Th. Richter, and W. Vogel. Nonclassicality criteria in terms of moments. *Phys. Rev. A*, 71:011802(R), Jan 2005.
- [34] A. Kenfack and K. Życzkowski. Negativity of the wigner function as an indicator of non-classicality. *J. Opt. B*, 6:396, 2004.
- [35] S. De Bièvre, D. B. Horoshko, G. Patera, and M. I. Kolobov. Measuring nonclassicality of bosonic field quantum states via operator ordering sensitivity. *Phys. Rev. Lett.*, 122:080402, Feb 2019.
- [36] Shuro Izumi, Masahiro Takeoka, Kazuhiro Ema, and Masahide Sasaki. Quantum receivers with squeezing and photon-number-resolving detectors for m -ary coherent state discrimination. *Phys. Rev. A*, 87:042328, Apr 2013.
- [37] Stephen M. Barnett, Lee S. Phillips, and David T. Pegg. Imperfect photodetection as projection onto mixed states. *Optics Communications*, 158(1):45–49, 1998.

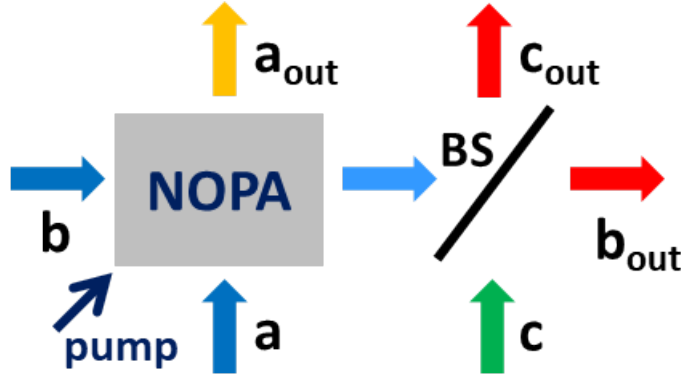


Figure 1: Schematic illustration of the proposed setup: a Nondegenerated Optical Parametric Amplifier (NOPA) with classical pump (strength s and phase ϕ), having \hat{a} and \hat{b} input modes. One of the output modes feeds a beamsplitter (BS), which has a second input mode, \hat{c} . Photodetectors may be placed in pairs in the output modes, either in \hat{b}_{out} and \hat{c}_{out} or \hat{a}_{out} and \hat{c}_{out} .

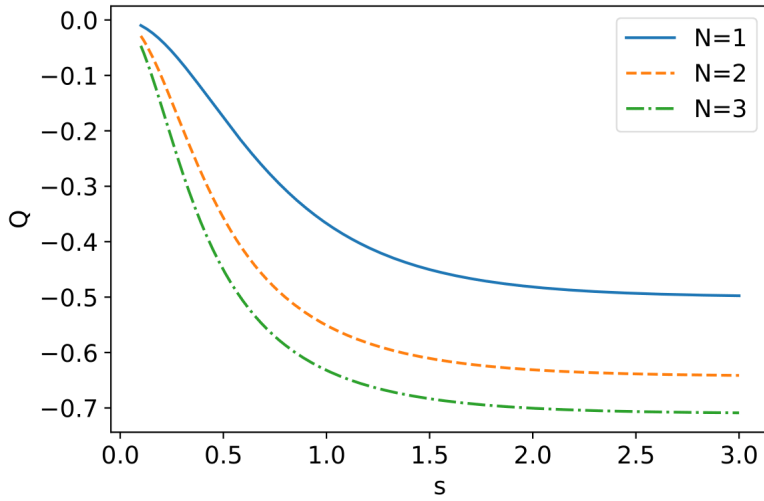


Figure 2: Mandel's Q parameter relative to state $|\Phi_a\rangle$ as a function of s for $\phi - \beta = \pi/2$ rad and $\theta = \pi/4$ rad.

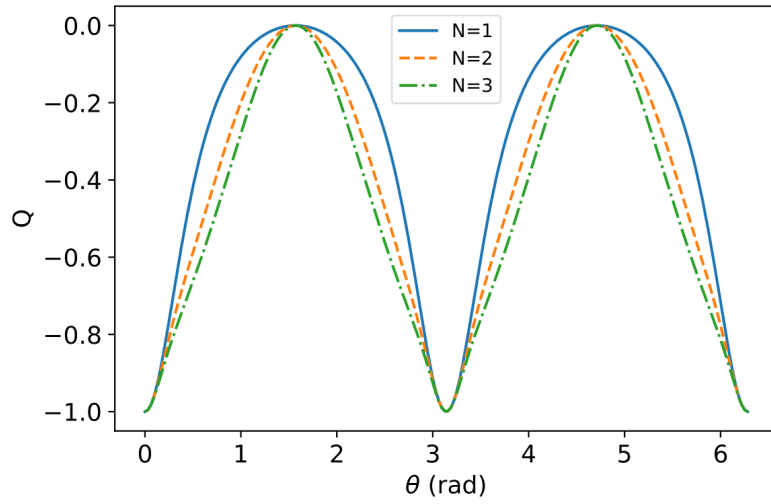


Figure 3: Mandel's Q parameter relative to state $|\Phi_a\rangle$ as a function of θ for $s = 0.5$ and $\phi - \beta = \pi/2$ rad.

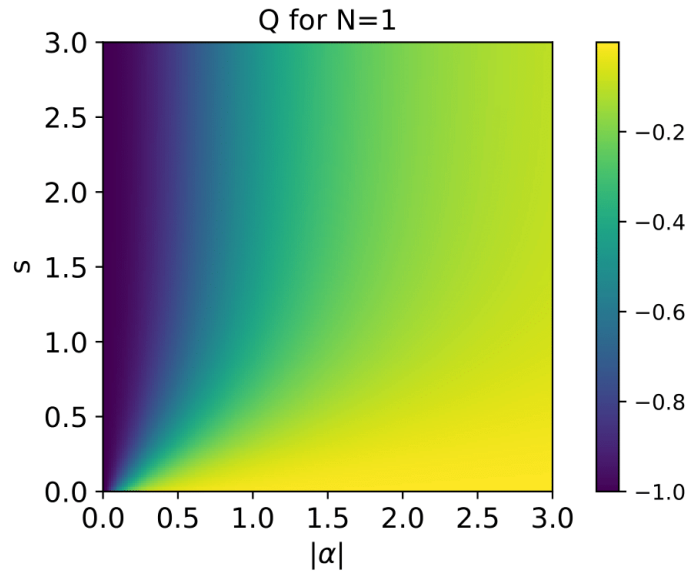


Figure 4: Mandel's Q parameter relative to state $|\Phi_a\rangle$ as a function of $|\alpha|$ and s , for $\theta = \pi/4$ rad, $\phi - \beta = \pi/2$ rad, and $N = 1$.

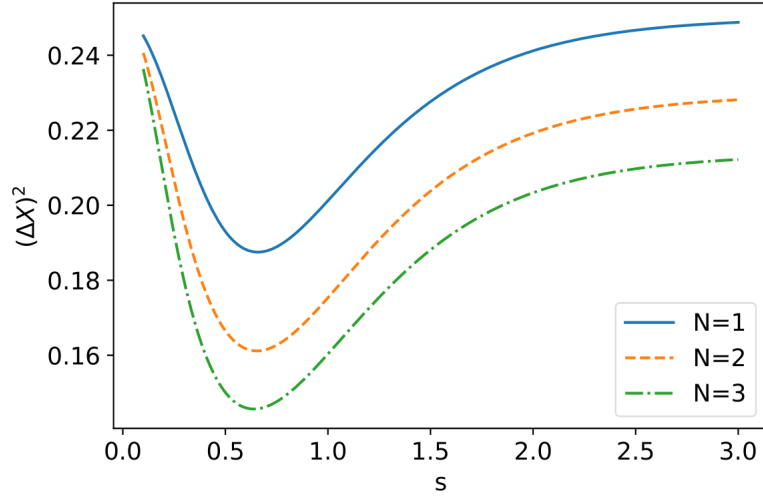


Figure 5: Variance of \hat{X} relative to state $|\Phi_\alpha\rangle$ as a function of s for $\phi - \beta = \pi/2$ rad and $\theta = \pi/4$ rad.

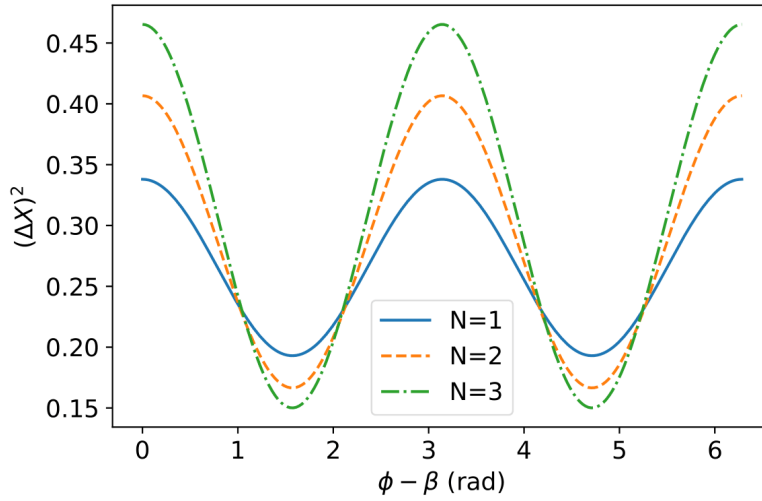


Figure 6: Variance of \hat{X} relative to state $|\Phi_\alpha\rangle$ as a function of $\phi - \beta$ for $s = 0.5$ and $\theta = \pi/4$ rad.

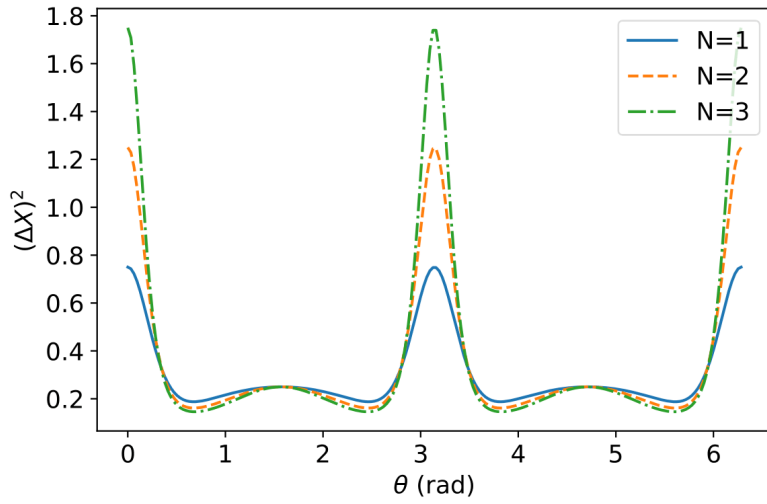


Figure 7: Variance of \hat{X} relative to state $|\Phi_a\rangle$ as a function of θ for $s = 0.5$ and $\phi - \beta = \pi/2$ rad.

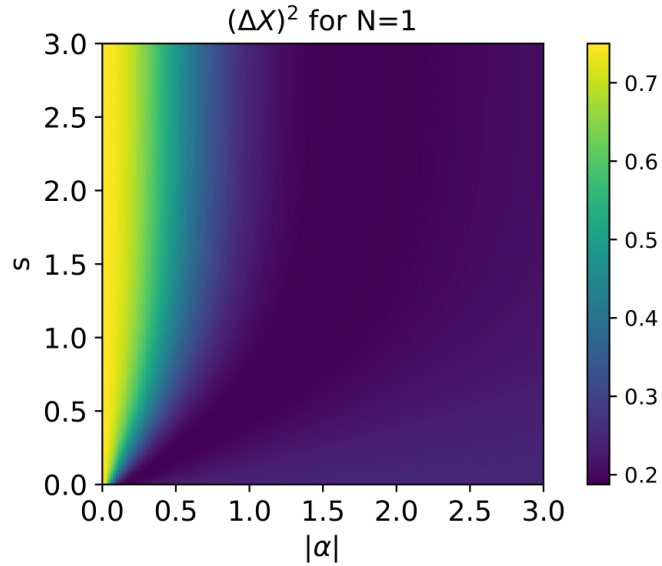


Figure 8: Variance of \hat{X} relative to state $|\Phi_a\rangle$ as a function of $|\alpha|$ and s , for $\theta = \pi/4$ rad, $\phi - \beta = \pi/2$ rad and $N = 1$.

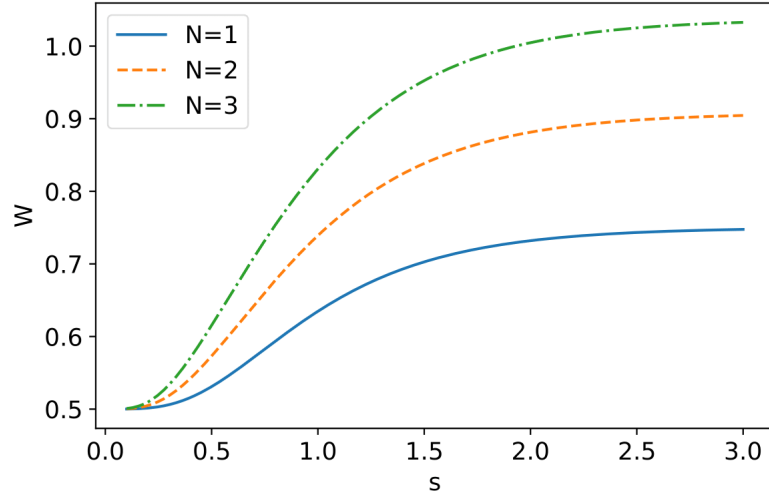


Figure 9: Skew information relative to state $|\Phi_a\rangle$ as a function of s for $\phi - \beta = \pi/2$ rad and $\theta = \pi/4$ rad.

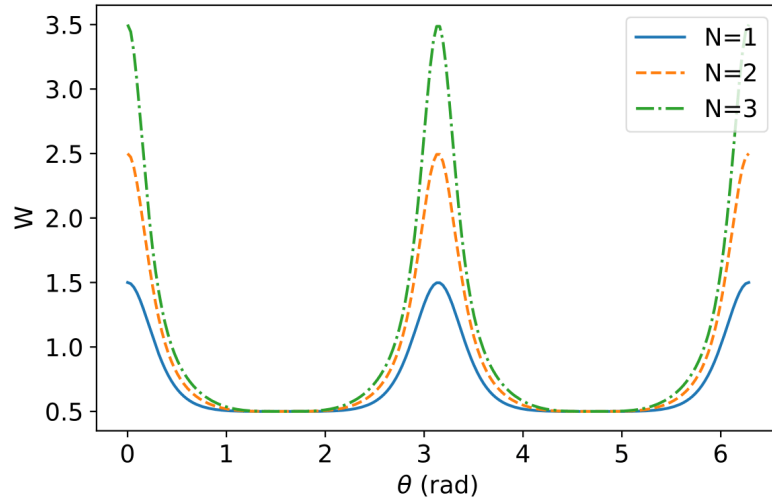


Figure 10: Skew information relative to state $|\Phi_a\rangle$ as a function of θ for $s = 0.5$ and $\phi - \beta = \pi/2$ rad.

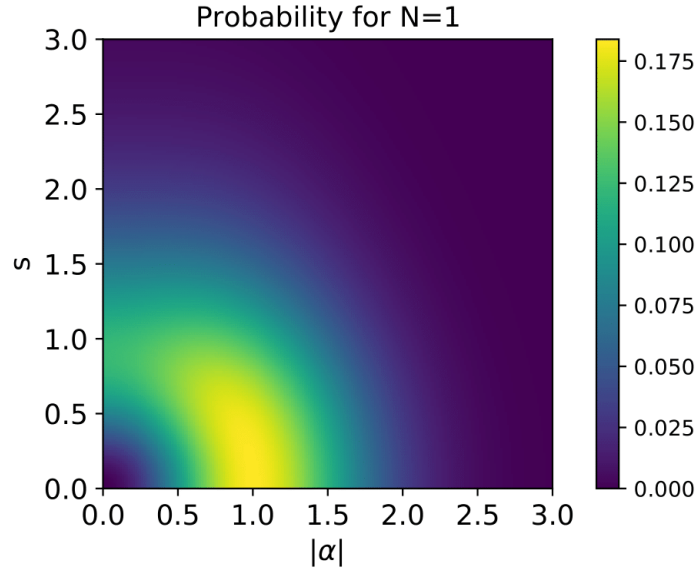


Figure 11: Probability of generation of state $|\Phi_a\rangle$ as a function of $|\alpha|$ and s , for $N = 1$, $\theta = \pi/4$ rad and $\phi - \beta = \pi/2$ rad.

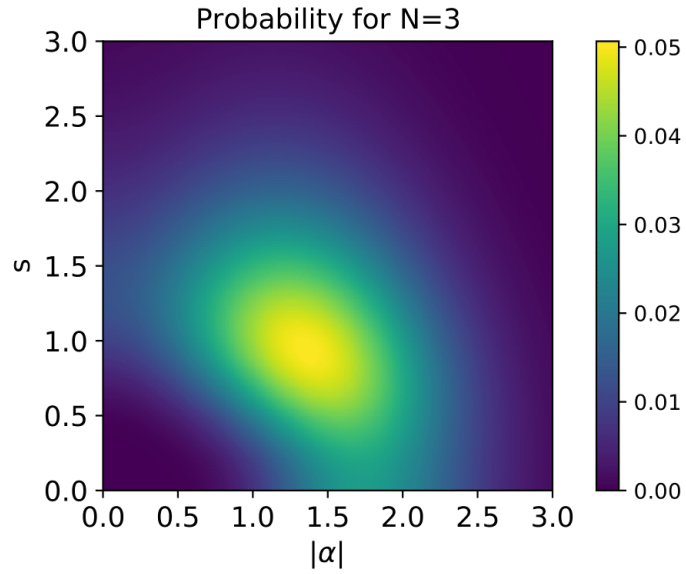


Figure 12: Probability of generation of state $|\Phi_a\rangle$ as a function of $|\alpha|$ and s , for $N = 3$, $\theta = \pi/4$ rad and $\phi - \beta = \pi/2$ rad.

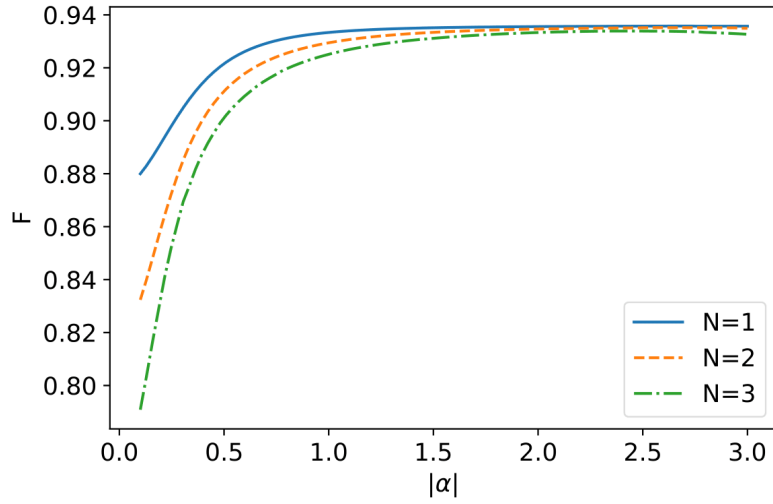


Figure 13: Fidelity as a function of $|\alpha|$ for $s = 0.5$, $\theta = \pi/4$, and $\phi - \beta = \pi/2$ rad. Here $\eta = 0.7$ and $\nu = 10^{-4}$.

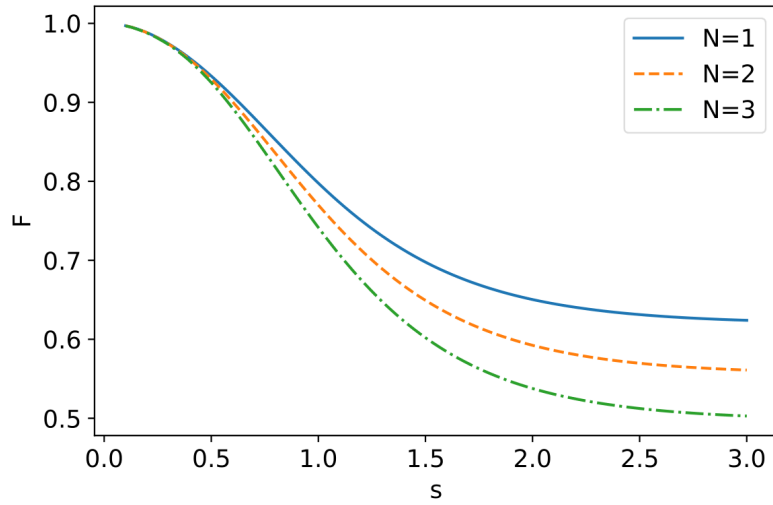


Figure 14: Fidelity as a function of s for $|\alpha| = 1$, $\theta = \pi/4$ and $\phi - \beta = \pi/2$ rad. Here $\eta = 0.7$ and $\nu = 10^{-4}$.